



# An experimental investigation into the warm deep-drawing process on laminated sheets under various grain sizes



Ehsan Afshin, Mehran Kadkhodayan \*

Department of Mechanical Engineering, Ferdowsi University of Mashhad, Mashhad, Iran

## ARTICLE INFO

### Article history:

Received 27 April 2015

Received in revised form 9 July 2015

Accepted 11 July 2015

Available online 4 August 2015

### Keywords:

Warm deep-drawing

Laminated sheet

Load–displacement curve

Grain size

Blank holder force

## ABSTRACT

It has been proved by many researchers that increasing the temperature in warm deep-drawing process of single layer sheets decreases the forming load, however, this phenomenon is not necessarily the case in warm deep-drawing process of laminate sheet. The objective of the present paper is to carry out a comprehensive investigation on warm deep-drawing process on laminated sheets experimentally. Based on the results of this study, it can be observed that by raising the temperature, variation of forming load more depends on blank holder force (BHF). In this study, thinning and wrinkling in Al 1050/St 304 and Al 5052/St 304 samples for each layer in warm deep-drawing process are evaluated individually. In addition, the effects of various grain sizes, blank temperatures and sequence layer on forming load are investigated. In order to carry out a comprehensive survey of warm deep-drawing; three blank temperatures namely, 25 °C, 100 °C and 160 °C are examined. Furthermore, to achieve various grain sizes, the aluminum sheets are annealed at 350 °C, 400 °C and 450 °C for 1 h. Finally, several tests are conducted to obtain the influences of grain size on some material characteristics such as stress, elongation and friction coefficient.

© 2015 Elsevier Ltd. All rights reserved.

## 1. Introduction

Nowadays, warm deep-drawing process, as one of the most applicable sheet metal forming processes, has been attracting more and more attention because of their application advantages such as manufacturing of complex shape, improved formability, reduced production time and controlled plastic flow. Because of re-crystallization, the temperature is one of the notable points during the forming process. The temperature during the warm deep-drawing should be kept below the re-crystallization temperature. The temperature affects the material behavior during the process and accuracy of finished parts. In comparison to hot forming processes, warm forming requires higher forces for deformation because of the greater material flow stress [1,2].

Due to a wide range of application and unique characteristics of laminates sheet such as high strength, low density, damping covering structures and corrosion resistibility researcher are paying more attention to laminated sheets. Therefore, they are used in various industrial fields such as aerospace, automobile, chemical and electrical industries. A laminated sheet consists of two or more metals with different material combinations and different thicknesses. In general, laminated sheets can be made by several processes, such as explosive bonding, adhesive bonding or cold and hot roll bonding. The laminated sheets formed by warm deep-drawing process can be used in manufacturing of parts

with different inner and outer conditions for instance, corrosion, wear resistance and thermal and electrical conductivities [3,4].

In recent years, many researchers have dealt with deep-drawing process of laminated sheets. Despite that, the investigations carried out on laminated sheet deformation during the deep drawing process, were surveyed only in room temperature. Deep-drawing process of laminated sheet Fe/Al was simulated by Takuda et al. [5]. The fracture initiation and the forming limit were successfully predicted by using the ductile fracture criterion and compared with experimental observations. They found that the drawing ability and LDR of aluminum alloy sheet can be improved by laminated sheet where Fe layer was set on the punch side. Parsa et al. [6] investigated the behavior of Al/St laminated sheets during deep-drawing, direct and reverse redrawing processes by simulations and experiments. It can be found that to achieve the highest LDR in direct and reverse redrawing, the thickness ratio should be about 1/3 (one-layer of aluminum and three-layer of stainless steel) and the setting conditions were opposite to each other. The wrinkling of laminated sheets (Al/St) in the deep-drawing process, were studied through an analytical method, numerical simulations and experiments by Morovvati et al. [7]. Moreover, influence of stacking sequence of the layers on forming load and wrinkling were demonstrated. The forming force where the aluminum layer was stuck to the upper layer was greater than the one the stainless steel layer was stuck to the upper layer. Nevertheless, thinning and lubrication effect on forming load were not surveyed. Influences of several parameters in deep-drawing process of laminated sheets (Steel/Brass), including stacking sequence of layers, lubrication and thinning were presented by

\* Corresponding author.

E-mail address: [kadkhoda@um.ac.ir](mailto:kadkhoda@um.ac.ir) (M. Kadkhodayan).

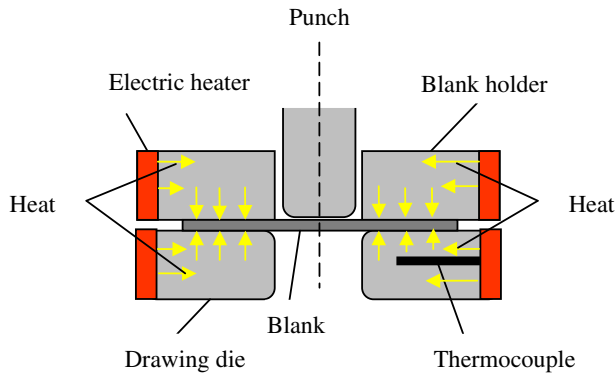


Fig. 1. Schematic representation of the equipment for the deep-drawing test.

Atrian and Fereshteh-Saniee [8]. They showed that the specimens with steel in the upper layer need higher forming load for deformation compared to those of brass in the upper layer. Rajabi et al. [9] investigated the deep-drawing process of two thermoplastic metal-composite laminates. They showed that the BHF had a significant effect on the wrinkling of laminates while the temperature had only a significant effect on the maximum forming load.

Nowadays, aluminum alloys are desirable for aerospace and automotive industry because of: (i) excellent high-strength to weight ratio, (ii) superior corrosion resistance, (iii) high weldability, and (iv) recyclability of alloys (for instance, recycling potential of the aluminum alloy products is much better than the ferrous metals). However, the formability and surface quality of final products are diminished when those are produced in room temperature. Consequently, warm forming is used to enhance the formability and the surface quality [10].

Warm deep-drawing for aluminum alloys has already been reported by many researchers. Bolt et al. [11] conducted warm deep-drawing experiments on various aluminum alloys (1050, 5754-O and 6016-T4) between 100 C and 250 C using box shaped and conical rectangular dies. Their study showed that raising temperature increased formability. Takuda et al. [12] reported the simulation results for cylindrical deep-drawing of aluminum alloy at elevated temperatures and observed that the necking site and forming limits were successfully predicted by simulation. The warm deep-drawing on aluminum sheet was investigated by Van den Boogaard and Huetink [13]. The behavior of aluminum was modeled using Hill 48 yield, von Mises criterion and Bergstrom hardening model and it was concluded that the Hill 48

Table 1  
Dimensions of various parts of the deep-drawing die set.

| Dimension                    | Value (mm) |
|------------------------------|------------|
| Punch diameter               | 65.5       |
| Die inner diameter           | 70         |
| Die outer diameter           | 153.5      |
| Punch and die profile radius | 5          |
| Blank holder inner diameter  | 67         |
| Blank holder outer diameter  | 164        |
| Clearance                    | 2.25       |

Table 2  
Chemical composition (wt.%) of aluminum alloys and stainless steel.

| Element | Al 1050 | Al 5052 | St 304 |
|---------|---------|---------|--------|
| Si      | 0.12    | 0.25    | 0.44   |
| Fe      | 0.28    | 0.40    | 70.55  |
| Cu      | 0.02    | 0.10    | 0.14   |
| Mn      | 0.02    | 0.10    | 1.38   |
| Mg      | 0.02    | 2.82    | –      |
| Zn      | 0.011   | 0.10    | –      |
| Ti      | –       | 0.15    | –      |
| Cr      | –       | 0.10    | 19.97  |
| AL      | 99.49   | 95.98   | –      |
| V       | –       | –       | 0.12   |
| Ni      | –       | –       | 7.00   |

criterion could not suitably predict the thinning. Palumbo and Tricaico [14] clearly demonstrated that the formability with a partial heating in die or blank holder area was much better than those obtained with homogeneously heated tools. In addition, the results showed that the temperature in the blank center strongly affects the formability and punch force. Nevertheless, distribution of thickness was not considered. Kim et al. [15] developed analytically a non-isothermal model for warm deep-drawing using various punch speeds and temperatures. The punch speed and temperature had noticeable effect on LDR and thickness distribution. Therefore, with increasing the punch speed LDR decreased. Furthermore, when the punch and die temperatures were 25 C and 180 C respectively, thickness distribution was more uniform than when they were 180 C. The effects of blank holder force on the wall thickness distribution and wrinkles in deep-drawing process of Al 1050 were investigated by Ibrahim Demirci et al. [16]. Their studies showed that for the blank holder force between 0.65 MPa and 10 MPa, the process was carried out

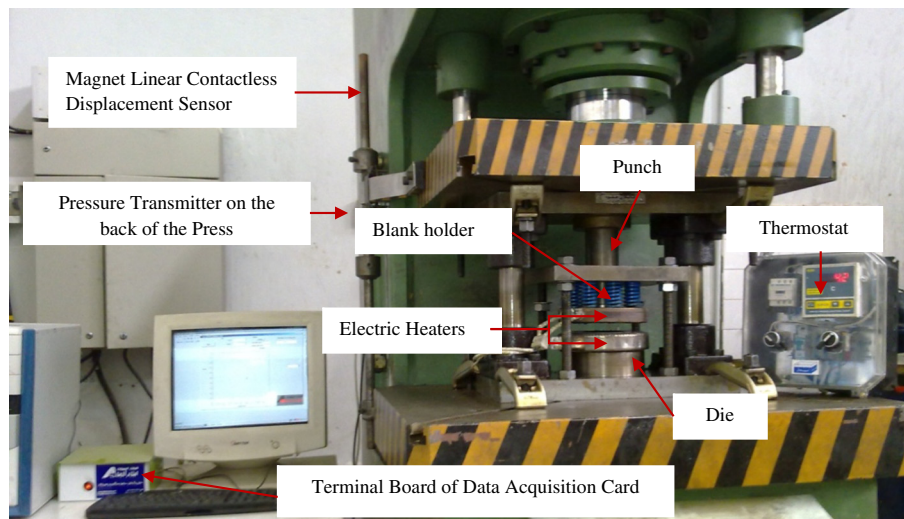


Fig. 2. Experimental test equipment.

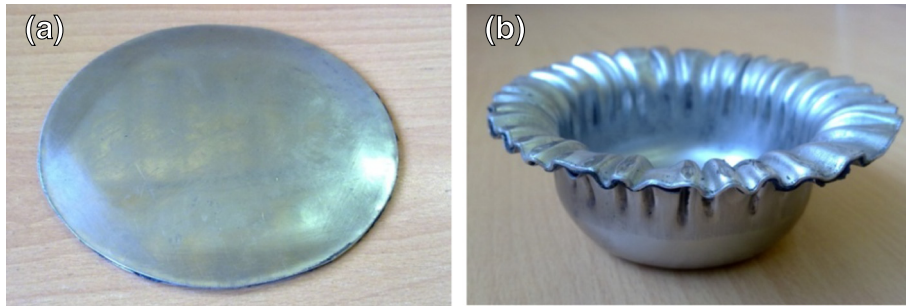


Fig. 3. Sample of laminated sheet (a) before forming, and (b) after forming.



Fig. 4. PLM microstructure of Al 5052 specimen with three annealing temperatures of (a) 350 C, (b) 400 C, and (c) 450 C.

without wrinkling and tearing. Sherbiny et al. [17] observed the influences of punch and die radius on thinning and residual stresses of sheet metal in the deep-drawing process experimentally. Furthermore, they demonstrated that the lower friction coefficient ( $\mu = 0-0.3$ ), was more suitable to reduce the thinning of the cup. Prediction of the forming results such as spring back, thickness distribution and thinning of the sheet metal with the finite element analysis simulation (FEAS) surveyed by Zein [18]. They recommended geometry of die shoulder and amount of punch nose radius in order to reduce

spring back. Furthermore, special BHF was recommended to avoid more thinning and spring back. The behavior of two Al–Mg–Si alloys including earring, thinning and forming load during the warm deep-drawing process at room temperature and 250 C was surveyed by Gosh et al. [19]. Moreover, the effect of temperature, ram speed and drawing ratio were also investigated. Among the studied parameters, the effect of temperature was significant on the force-displacement response. Additionally, the ear height and forming load decreased when the temperature rose to 250 C.

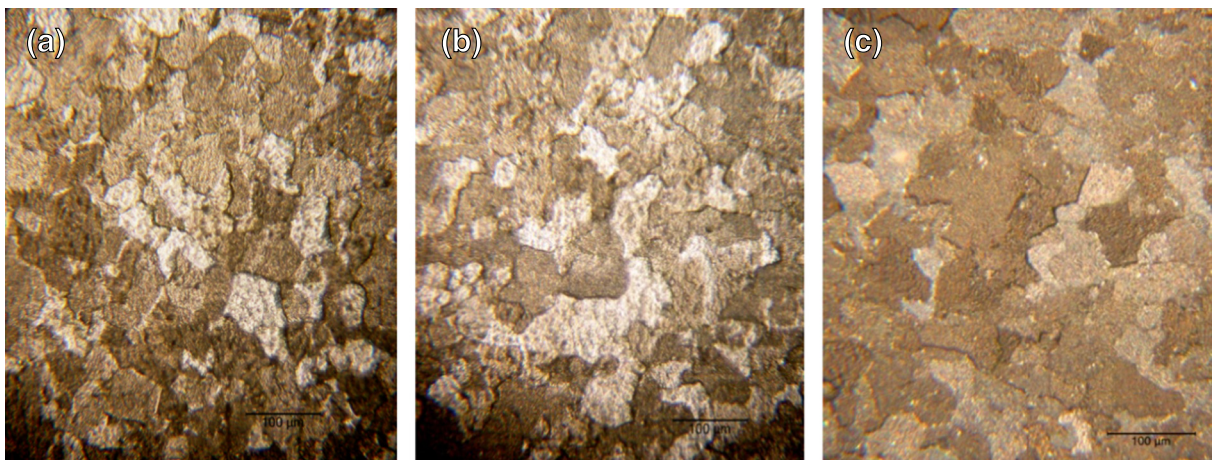


Fig. 5. PLM microstructure of Al 1050 specimen with three annealing temperatures of (a) 350 C, (b) 400 C, and (c) 450 C.

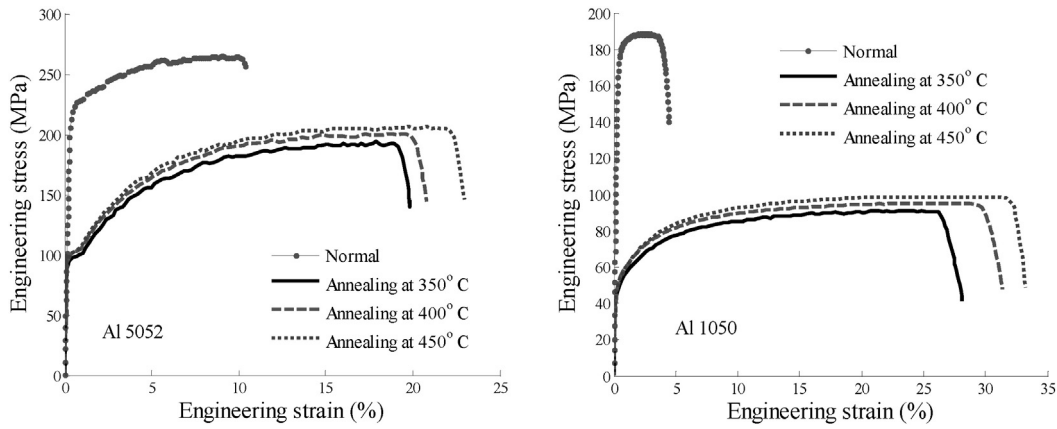


Fig. 6. Engineering stress–strain behavior of Al 5052, and Al 1050 for annealing at various temperatures.

Moreover, stainless steel sheets are increasingly used for producing various parts in the kitchen, vessels, transformation, etc., because of their high corrosion-resistivity and beautiful appearance. Stainless steel 304 is commonly used for forming products because of noticeable formability. Austenite in St 304 is unstable and transformed to martensite during cold forming process. This transformation leads to enhancement of the work-hardening rate, which is desirable for the high formability because of the delayed cracking. On the other hand, to obtain suitable deep cups by deep-drawing, several redrawing processes are necessary which lead to increase of time and cost of production. During cold forming the high content of martensite causes accumulated strain in forming process, brings an increase in forming load and decrease in corrosion resistivity, magnetization and delayed cracking. One way to prevent martensitic transformations is warm forming, because the martensitic transformation decreases with increasing temperature [1].

To improve some criteria like LDR, thinning, spring back and plastic flow many studies have been presented on stainless steel using warm deep-drawing process. Takuda et al. [20] conducted both simulation and experimental studies on St 304 under warm forming to survey

drawing ability. Their study showed that the limiting drawing ratio reached to the desirable amount of 2.7 at 150 C, while its greatest possible amount was 2.0 at room temperature. The influences of several parameters such as punch speed, friction coefficient and temperature on final parts of St 304 in warm deep-drawing process were demonstrated by Singh et al. [21]. It was clear from their study that forming load reduced with decreasing friction coefficient and punch speed. Moreover, effect of temperature on thinning, LDR and forming load was appreciable. Ethiraj and Kumar studied the St 304 deep-drawing process through finite element simulation [22] and empirical observation [23]. They observed that raising the temperature up to 300 C leads to (i) no tearing or necking in the final cup shapes, (ii) reducing the required drawing load by 40% and (iii) a maximum 4% and 9% of thinning and thickening, respectively, of the specimen. They also revealed the microstructures of the analyzed sample before and after forming.

Table 4  
Mechanical properties for Al 1050, and 5052.

| Type               | $S_y$ (MPa) |         | $S_{uts}$ (MPa) |         | Elongation (%) |         |
|--------------------|-------------|---------|-----------------|---------|----------------|---------|
|                    | Al 1050     | Al 5052 | Al 1050         | Al 5052 | Al 1050        | Al 5052 |
| Normal             | 173.1       | 223.8   | 189.2           | 266.5   | 4.5            | 10.37   |
| Annealing at 350 C | 46.4        | 98.2    | 91.2            | 193.9   | 28.1           | 19.8    |
| Annealing at 400 C | 48.3        | 101.2   | 95.1            | 200.8   | 31.2           | 20.7    |
| Annealing at 450 C | 49.1        | 102.1   | 98.5            | 206.8   | 33.3           | 23      |

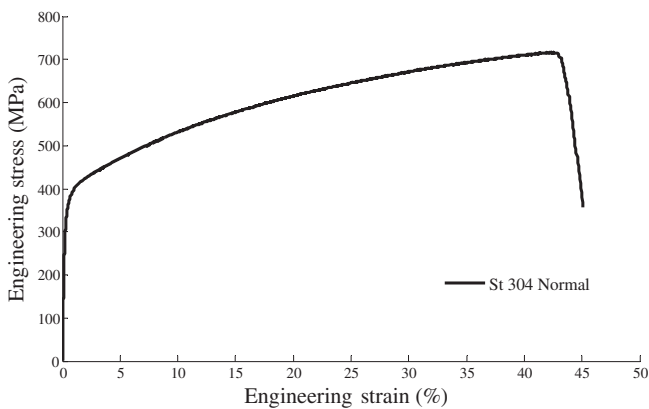


Fig. 7. Engineering stress–strain behavior of stainless steel 304.

Table 3  
Grain size for aluminum alloys.

| Annealing temperature | GS for Al 5052 ( $\mu\text{m}$ ) | GS for Al 1050 ( $\mu\text{m}$ ) |
|-----------------------|----------------------------------|----------------------------------|
| 350 C                 | 10                               | 37                               |
| 400 C                 | 12                               | 40                               |
| 450 C                 | 14                               | 44                               |



Fig. 8. The drawn product sectioned diametrically using a water jet machine for evaluation of thickness strain.

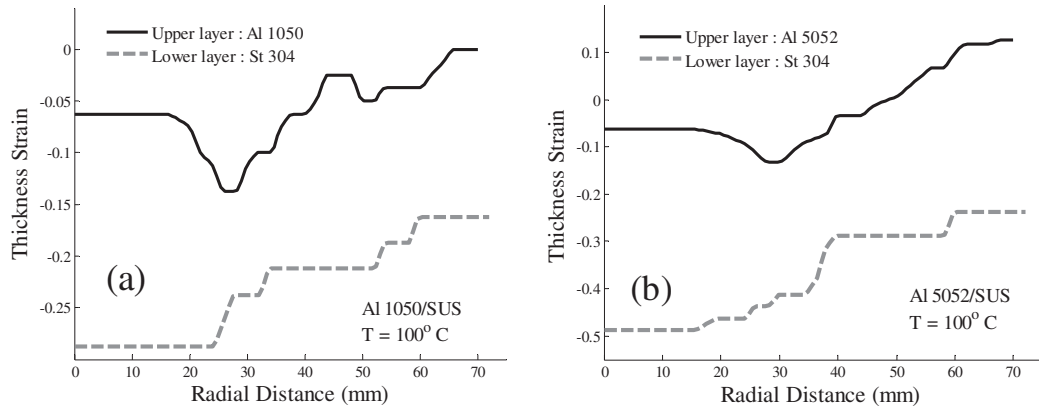


Fig. 9. The distributions of the thickness strain for each layer individually of (a) Al 1050/SUS (BHF = 15 kN), and (b) Al 5052/SUS (BHF = 18 kN).

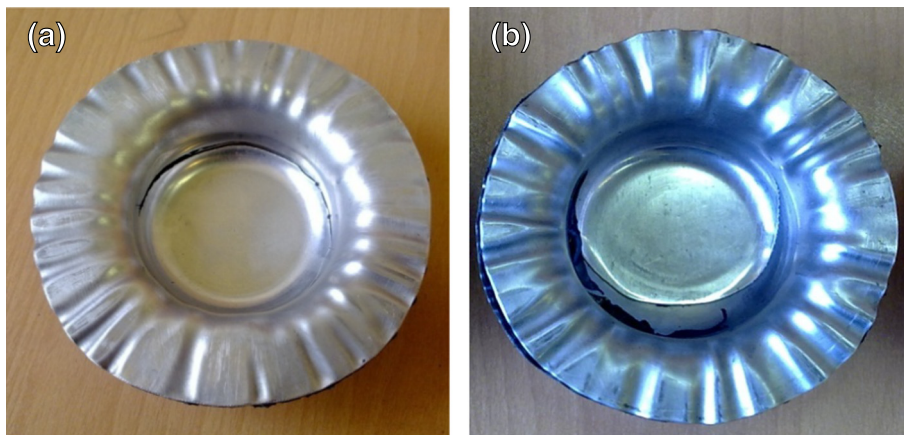


Fig. 10. Tearing took place at the punch profile radius region for (a) Al 1050 (BHF = 17 kN, T = 100 C), and (b) Al 5052 (BHF = 19 kN, T = 100 C).

Annealing and grain size are main factors in deep-drawing in order to improve the quality of product, formability, wrinkle pattern, forming load, limit drawing ratio and forming limit diagram (FLD). The grain size is strongly reliant on annealing and re-crystallization. Moreover, the effect of cold rolling is omitted by heat treatment; therefore, properties of metal are changed. Bacroix et al. [24] performed some tensile test to clarify influences of grain size and texture on the formability of Al 1050. In addition, the macroscopic stress–strain curves have also been

analyzed. Their study made it clear that re-crystallization took place already at the lowest investigated temperature of 280 C; moreover, the macroscopic response of the tested materials strongly depended on their texture. The effects of initial grain size of commercial pure aluminum on hot deformation behavior were investigated using hot compression tests by Rezaei Ashtiani et al. [25]. The results indicated that the initial grain size had notable effect on the flow stress. Flow stress also decreased when the grain size decreased from 450 to 50 μm.

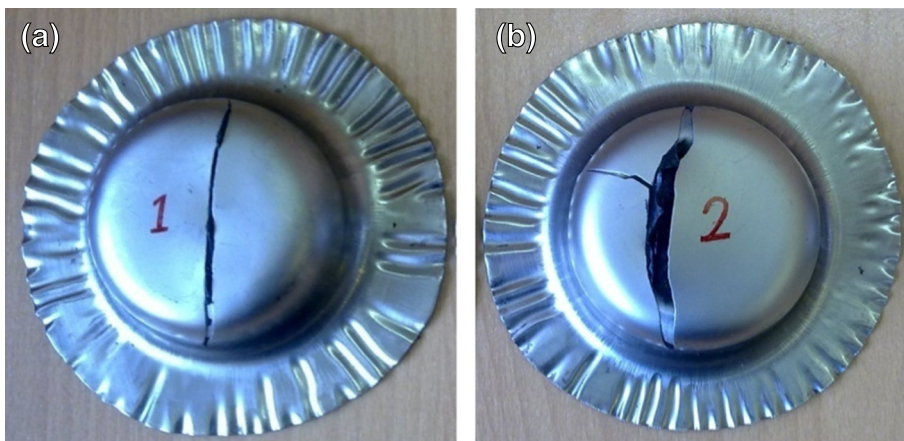


Fig. 11. Tearing took place central area of cup for St 304 in (a) Al 1050/SUS sample (BHF = 17 kN, T = 100 C), and (b) Al 5052/SUS sample (BHF = 19 kN, T = 100 C).

**Table 5**

Some characteristics of wrinkles for all layers in Al 1050/SUS ( $T = 100\text{ C}$ , BHF = 15 kN), and Al 5052/SUS ( $T = 100\text{ C}$ , BHF = 18 kN) samples.

| Characteristics of Wrinkle | Al 1050/SUS |        | Al 5052/SUS |        |
|----------------------------|-------------|--------|-------------|--------|
|                            | Al 1050     | St 304 | Al 5052     | St 304 |
| Average height (mm)        | 2.15        | 2.45   | 1.85        | 2.05   |
| Number                     | 26          | 28     | 26          | 29     |
| Maximum height (mm)        | 2.60        | 2.60   | 2.40        | 2.40   |
| Minimum height (mm)        | 0.40        | 0.80   | 0.50        | 0.90   |

The aim of the present work is to investigate the forming of laminated sheets including Al 1050/St 304 and Al 5052/St 304 by warm deep-drawing process. Because of temperature and complex plastic deformation mechanisms of laminated sheets which it is most likely due to different mechanical properties and formability of each layer, studies on wrinkling, thinning and forming load of laminated sheets in warm deep-drawing process have not been conducted so far. One of the interesting subjects in the current study is thickness distribution for each layer. Usually tearing for single layer sheets is occurred on punch radius, but tearing for stainless steel sheets are occurred on central area of cup. In addition, the effect of raising temperature on warm deep-drawing of laminate sheets is very complex because it enhances the formability which leads to reducing forming load; nevertheless, it increases the friction coefficient which leads to increasing forming load. This study made it clear that how these effects can be controlled to achieve desirable features. Effect of growth of grain size in aluminum sheets on

load–displacement curves, friction coefficient and mechanical properties are another parts of this study.

In summary, the objectives are to: (1) perform a heat treatment to achieve to various grain sizes on aluminum alloys 1050 and 5052, and also reveal their microstructures (2) conduct several tests to obtain the influences of grain size on some parameters such as stress, elongation and friction coefficient, (3) determine thinning, tearing and wrinkling in Al 1050/St 304 and Al 5052/St 304 samples for each layer separately, and (4) experimentally understand the effects of various parameters such as temperature, grain size, BHF and layers stacking sequence on the forming load in warm deep-drawing process on laminated sheets.

## 2. Experimental procedure

### 2.1. Warm deep-drawing equipment description

The scheme of the experimental equipment used for warm deep-drawing is illustrated in Fig. 1. The test rig consists of a draw die flange with circular shape, a blank holder, 8 springs which provide blank holder force (BHF), punch and heat equipment, Fig. 2. Moreover, some features of test rig are shown in Table 1. The test equipment is specially designed, so that warm deep-drawing operations can be performed at various temperatures. Die and punch are composed of a set of forming tools made of SPK steel and blank holder also is made of MO40 steel. To increase the temperature, two annular electrical heaters with 1400 W power are utilized. The annular electrical heaters are set on

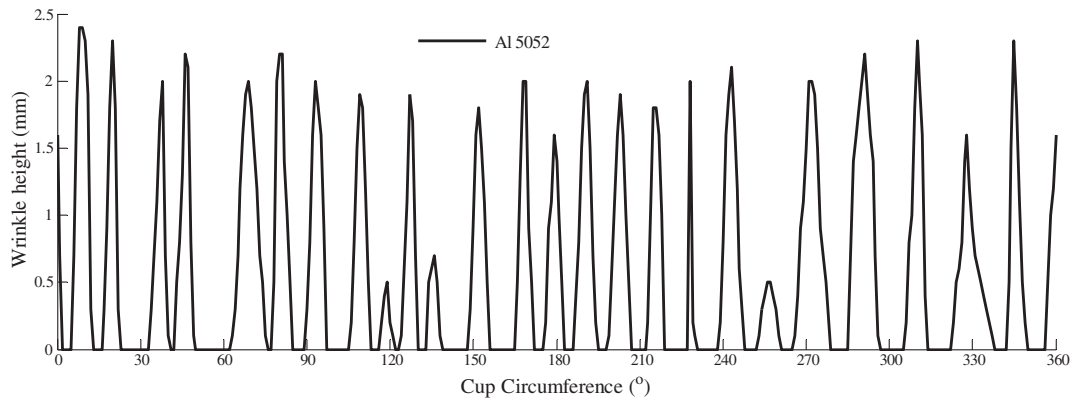


Fig. 12. Distribution of wrinkle for Al 5052 on Al 5052/SUS sample (BHF = 18 kN,  $T = 100\text{ C}$ ).

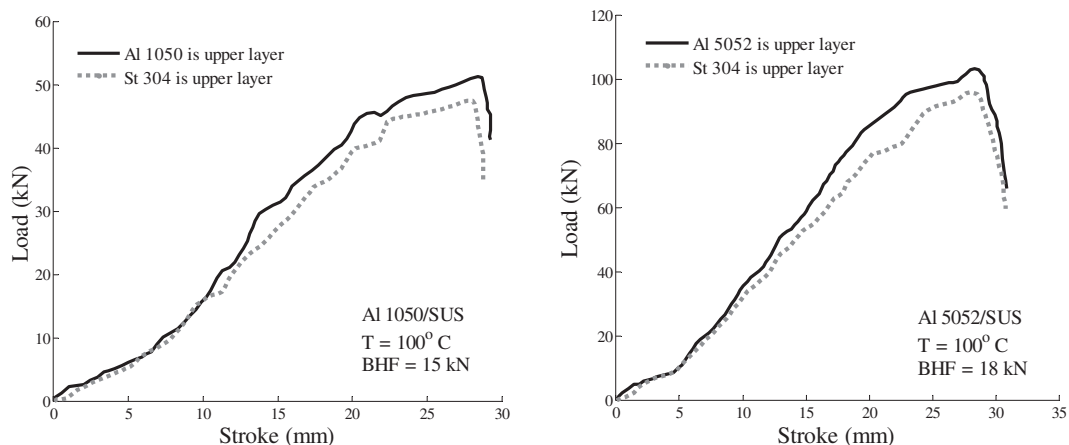


Fig. 13. Effect of layer stacking sequence on the load–displacement curves for Al 1050/SUS and Al 5052/SUS.

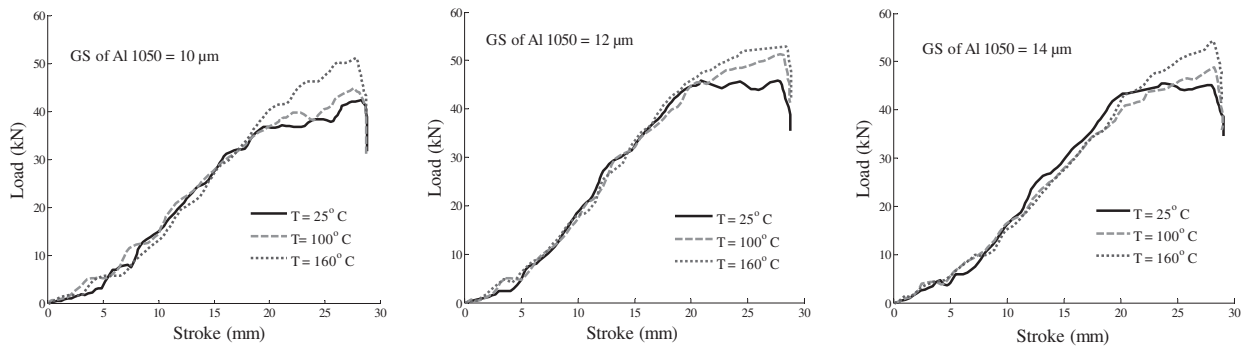


Fig. 14. Effect of various temperatures on load–displacement curve for specimen Al 1050/SUS when BHF = 15 kN.

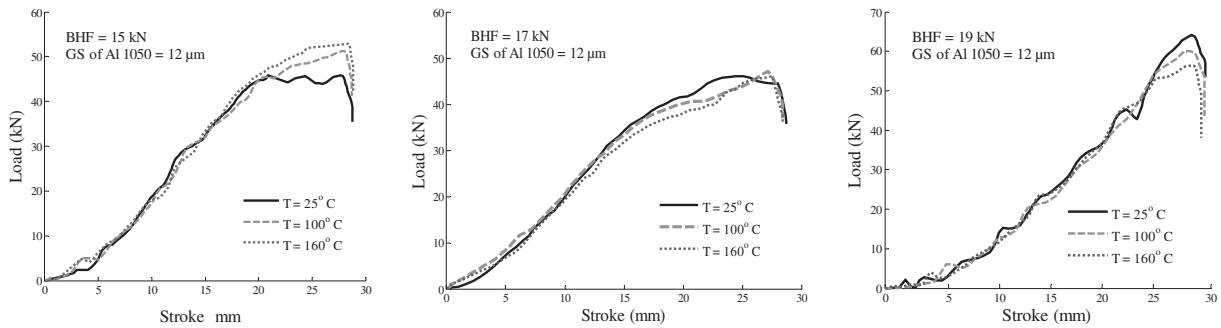


Fig. 15. Effect of various BHF on load–displacement curve for specimen Al 1050/SUS.

outer circumference of drawing die and blank holder. The heaters heat the drawing die and blank holder; as a result, the blank is heated but the blank has not direct contact with the heaters. In addition, a thermocouple is placed in die and to control the temperature a digital thermostat with the precision of 1 C is used. The required time to reach the temperature of 160 C is about 30 min. Deep-drawing of laminated sheet is carried out using a 60-ton hydraulic press. The punch speed of the press is 540 mm/min. To measure the force of forming process, a pressure sensor is installed on the hydraulic press which transforms the pressure to electric current. In addition, to measure the punch displacement a linear magnetic displacement sensor with the accuracy of micron level is used. All information comes to a data acquisition card and finally the Matlab software is used to analyze the obtained data.

## 2.2. Material and specimen preparation

The materials of layers are stainless steel 304 (SUS), aluminum alloy grades 1050 and 5052 which their chemical composition are given in Table 2. To perform more comprehensive investigation, two grades of aluminum alloys of 1050 and 5052 are combined with stainless steel 304 to make two different types of laminated sheets (Al 1050/St 304 and Al 5052/St 304). Taking forming load, die diameter and drawing depth into account the optimal diameter of the sheet is selected as 13.2 mm, and thickness for aluminum alloys 5052 and 1050 and stainless steel 304 are as 1, 0.8 and 0.4 mm, respectively. Loctite 5368 adhesive is applied to stick the sheets together because of some advantages such as high flexibility, medium to high initial strength and high heat resistant up to 300 C. Before gluing the two sheets together, all contact surfaces of the sheets are cleaned and sanded to remove impurities such as oxides and grease in order to enhance the bonding performance at specimen. The adhesive layer is uniformly distributed between sheets layer by rig press. Final thickness for Al 5052/SUS and Al 1050/SUS samples is 2 and 1.8 mm, respectively. The specimens before and after

forming are shown in Fig. 3. Stacking sequence in all specimens is in such a way that the aluminum sheet is set as the upper layer to be in contact with punch and the stainless steel sheet as the lower layer in contact with drawing die. In addition, process performed at dry condition.

## 2.3. Annealing

The grain size (GS) is a main factor in forming process that should be taken into account. Aluminum sheets used in this study are produced by rolling technology. This process affects mechanical properties of sheets such as strain hardening exponent, texture, grain size and grain orientation. In order to omit these effects, annealing heat treatment can be used. Influences of grain size on parameters such as flow stress, machining, friction coefficient and electrical properties are remarkable. Furthermore, annealing can remove any effect of strain hardening and improve material properties for forming [26]. Hence, samples are annealed at 350 C, 400 C and 450 C for 1 h. Then cooling process is carried out within the furnace for 24 h. To measure the grain size, samples are etched by (50 ml Poulton's reagent, 25 ml HNO<sub>3</sub>, 40 ml of solution of 3gr chromic acid per 10 ml of H<sub>2</sub>O) etchant. The best resolution of individual grains and microstructure of Al 5052 and Al 1050 are revealed by Polarized Light Microscope (PLM), see Figs. 4 and 5. The PLM microstructure results showed that the crystallization has taken place for all samples.

Table 6

Effect of different BHFs on plastic deformation and slide for Al 1050/SUS when T = 100 C and GS = 12 μm.

| BHF (kN) | Plastic deformation (mm) | Slide (mm) |
|----------|--------------------------|------------|
| 15       | 6                        | 27         |
| 17       | 13                       | 20         |
| 19       | 21                       | 12         |

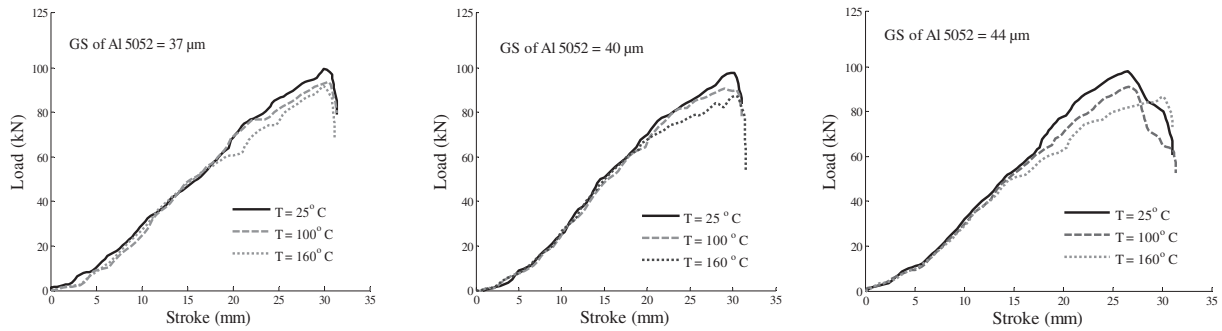


Fig. 16. Effect of various temperatures on load–displacement curve for specimen Al 5052/SUS when BHF = 18 kN.

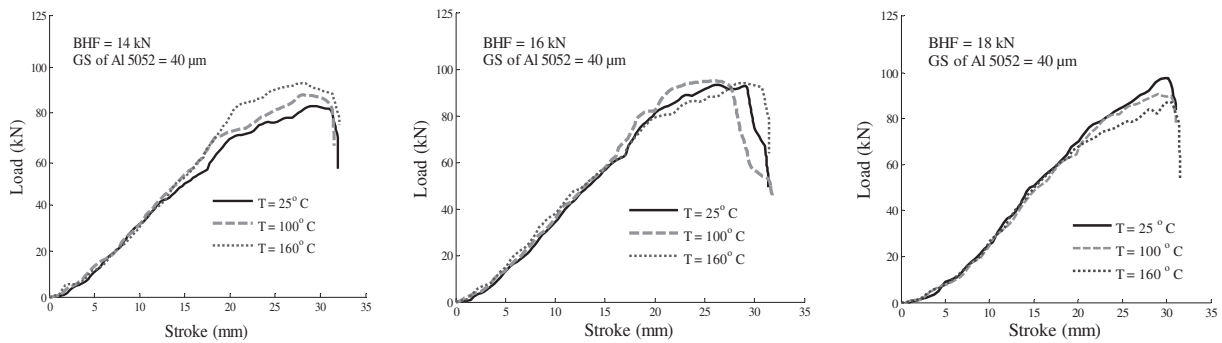


Fig. 17. Effect of various BHF on load–displacement curve for specimen Al 5052/SUS.

#### 2.4. Tensile test and flow stress

To determine the engineering stress–strain behavior of aluminum alloys and stainless steel 304 tensile tests are performed on a Zwick-Z250 uniaxial tensile test machine at room temperature. Tensile specimens of aluminum alloys 5052 and 1050 and stainless steel 304 are prepared to have the dimension with gauge length of 50.0 mm, width of 12.5 mm according to ASTM-0557 M-02 standard and are cut in the direction of 0 which conforms directly to the rolling direction. The tensile specimens of aluminum alloys 5052 and 1050 are annealed at the temperature conditions of 350 C, 400 C and 450 C for 1 h, after that they are cooled in the furnace for 24 h. This heat treatment process provides different grain sizes for samples which give the possibility to investigate the effect of grain size on the flow stress. The testing speed may affect the amounts of ultimate stress and yield stress when the grains size increase. The testing speed has significant effect on engineering stress–strain behavior as reported by Rezaei Ashtiani et al. [25]. According to the punch speed the tensile tests are carried out with testing speed of 0.002 (1/S). The engineering stress–strain curves for Al 1050 and Al 5052 and St 304 are illustrated in Figs. 6, and 7, respectively.

### 3. Results and discussion

#### 3.1. Effect of annealing on grain size and mechanical properties

The study showed that re-crystallization of aluminum alloys 5052 and 1050 occurred in the 350 °C. Regarding the PLM microstructure for Al 5052 and Al 1050, re-crystallization occurs in all samples. The grain sizes are measured based on the ASTM-E122-12 standard for various annealing temperatures and they are presented in Table 3. Effects of annealing on microstructure and grain size are illustrated in Figs. 4 and 5. It can be concluded that the grain size in Al 1050 and 5052 rises when annealing temperatures increase. In addition, the results of

engineering stress–strain curves showed that elongation, yield stress and ultimate stress increase with increasing the grain size, Table 4.

#### 3.2. Thinning and wrinkling

One of the most significant issues in warm deep-drawing process is thickness distribution of final product. Hence, for Al 1050/SUS and Al 5052/SUS samples, thickness strain variations of both layers are calculated individually. For this purpose, the drawn component is sectioned diametrically by means of a water jet machine, Fig. 8. Afterward, thickness of each layer at various positions from the centerline of the component is measured by using a micrometer. Consequently, the variation of thickness strain for each layer is specified in the radial direction, Fig. 9. The obtained results showed that the maximum thickness strain for both sheets; Al 1050 and Al 5052, are taken place in a radial distance of about 30 mm which is located almost in the region of punch profile radius. Hence, fracture occurs in that area of a drawn cup and this place is a high risk region for fracturing. Some tests conducted with higher BHF show that the ruptures on aluminum sheet take place on aforementioned area, Fig. 10. Moreover, it can be observed that the maximum thickness strain for St 304 sheet in both samples occurred at the central area of the cup, Fig. 11. As expected, tearing has taken place in the bottom of the cup where significant thickness strain occurs, Fig. 11.

Table 7  
Effect of different BHFs on plastic deformation and slide for Al 5052/SUS when T = 100 C and GS = 40 μm.

| BHF (kN) | Plastic deformation (mm) | Slide (mm) |
|----------|--------------------------|------------|
| 14       | 9                        | 22         |
| 16       | 14                       | 17         |
| 18       | 20                       | 11         |

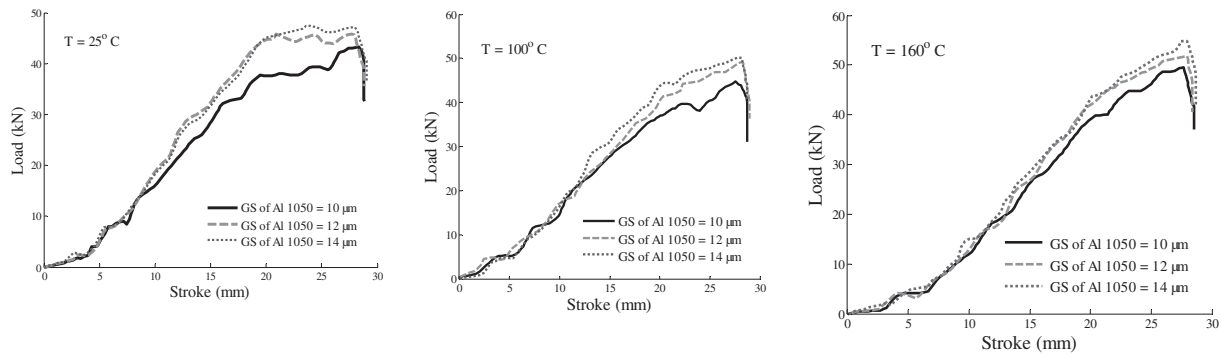


Fig. 18. Effect of various grain sizes of Al 1050 on load–displacement curve for specimen Al 1050/SUS when BHF = 15 kN.

Usually sheet drawing processes are designed in such a way that wrinkles can be prevented. The conditions for the onset of wrinkling are influenced by many factors such as stress ratios, anisotropy, geometry of the work piece and contact condition. During a sheet forming process, wrinkling can occur on the flange. In this study flange wrinkling for two different types of cups (Al 1050/SUS, and Al 5052/SUS) are surveyed, and it is also studied for each layer individually. Height and position of wrinkles are measured by metric dial indicator and dividing machine, respectively. Some characteristics of wrinkles including maximum and minimum heights, number of wrinkles and average wrinkles height for all layers in Al 1050/SUS and Al 5052/SUS are presented in Table 5. Fig. 12 shows a sample of wrinkling graph for Al 5052. It is seen that the average wrinkle height and number of wrinkles for stainless steel are more than those of aluminum sheets. Additionally, the maximum height of wrinkles for stainless steel sheets is equal to that of aluminum sheets. Nevertheless, the minimum height of wrinkles for stainless steel is more than that of aluminum. Compared to aluminum sheets, stainless steel ones have more number of wrinkles with less amplitude.

### 3.3. Effect of layer stacking sequence on load–displacement curve

The laminated sheet behavior in a forming process differs from a single layer sheet and depends on the layer sequence. Because of individual mechanical characteristics for each layer, changing of layer sequence leads to changing of some parameters like fracture, fatigue damage and load forming of the sample. Effects of layer sequences on load–displacement curves for Al 1050/SUS and Al 5052/SUS are demonstrated in Fig. 13. It is seen that the trend of variations for Al 1050/SUS sample when the order of layer changes, resembles to that of Al 5052/SUS sample. Moreover, the samples with stainless steel on upper layer require lower forming load rather than the samples with aluminum.

### 3.4. Effect of blank temperature on load–displacement curve

The effect of blank temperature on load–displacement curve is also investigated here. Therefore, some experiments with various blank temperatures namely, 25 C, 100 C and 160 C on specimens consisted of Al 1050 and stainless steel 304 (SUS) are performed. To make the results more reliable, the experiments carried out on three types of specimen with various grain sizes in Al 1050 sheet, Fig. 14. During the experiments the blank holder force is taken as 15 kN. As it is observed, one may see an unusual behavior here and the forming load increases when temperature increases for all type of specimens with different grain sizes. To explain this performance, two key factors with interaction effects have to be considered. The first one is the formability and plastic deformation of materials that rise with increasing temperature, therefore it decreases the required forming load [2,13]. The second one is the friction. In fact, raising the temperature causes the metal behaviors such as softening and adhesion change, therefore friction coefficient increases which raise the required forming load [27]. The experimental measurement of friction coefficient in warm deep-drawing process is presented by Coër [28]. The apparatus are specially designed to carry out tests with high temperatures. Results showed that the friction coefficient increase to about of 0.078 at room temperature and 0.118 at 200 C. The important issue here is how the effects of these parameters may be dominant. The experimental results show that the BHF plays a crucial role here. To clarify this phenomenon, three experiments with identical conditions except for BHF are performed, Fig. 15. It can be observed that choosing the lower BHF (near 15 kN) makes the friction effect to be dominant. In other words, when drawing process is performed with BHF of 15 kN, the effect of friction dominates rather than the formability and plastic deformation. Therefore, the forming of specimen in high temperature (160 C) needs more maximum load. In medium BHF (near 17 kN), the amount of forming load does not change with different blank temperatures significantly, that means both effects are nearly at the same level. Finally, using higher BHF (near 19 kN) causes the effect of formability to be prominent, for instance; when the BHF rises, the effect of formability and plastic deformation become dominant and different trends are observed. Hence, the specimen tested in low temperature (25 C) needs more maximum load.

One can go through this mechanism in more detail. Measuring diameter of specimen before and after the test showed that the specimen slid across the blank holder. In addition, the elongation and plastic

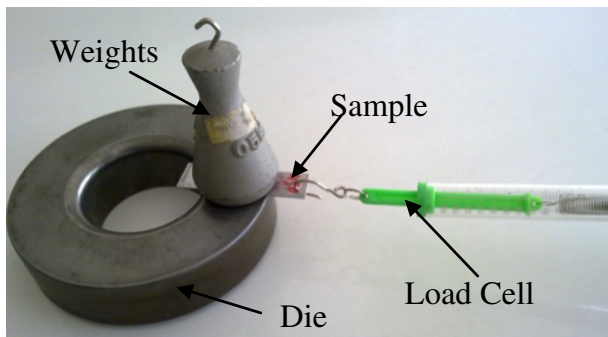


Fig. 19. Friction test apparatus.

Table 8  
Effect of grain size on friction coefficient.

| Sheets<br>Friction   | Various GS ( $\mu\text{m}$ ) for<br>Al 1050 |      |      | Various GS ( $\mu\text{m}$ ) for<br>Al 5052 |      |      |
|----------------------|---|------|------|---|------|------|
|                      | 10  | 12   | 14   | 37  | 40   | 44   |
| Friction coefficient | 0.30  | 0.37 | 0.41 | 0.28  | 0.34 | 0.37 |

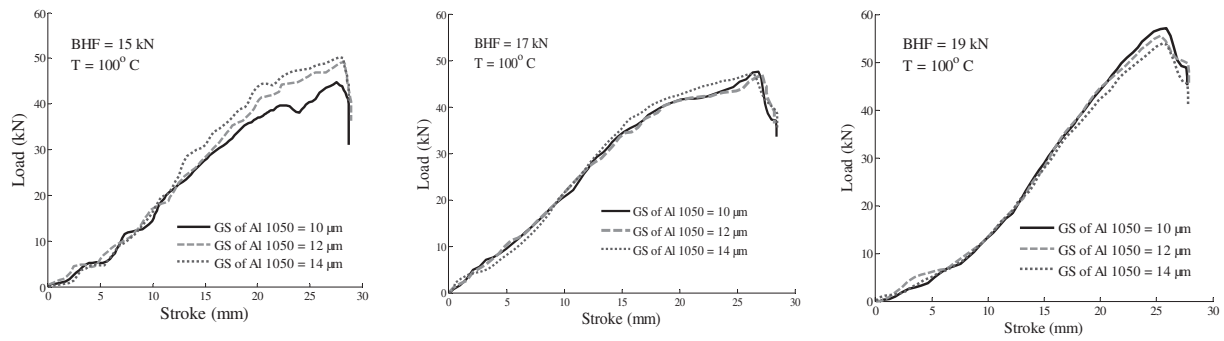


Fig. 20. Effect of various BHF on load–displacement curve for specimen Al 1050/SUS.

deformation are determined by lengths comparison. When lower BHF is used, the samples slid over the die profile radius more easily, and elongation and plastic deformation in samples are also reduced. Hence, because of long slide distance, the effect of friction which increases with rising of temperature becomes significant. However, using higher BHF leads to higher plastic deformation and less samples slide. Consequently, more formability and plastic deformation cause the forming load increases. Effects of different BHF on slide and plastic deformation for one sample of Al 1050/SUS are presented in Table 6.

In continuing, the experiments are performed on specimen made of Al 5052/SUS. Similar to Al 1050/SUS, experiments on Al 5052/SUS are performed on three samples with various grain sizes of Al 5052, Fig. 16. The obtained results are similar to ones of Al 1050/SUS and BHF plays a crucial role in load–displacement curves behavior. In higher BHF (18 kN), it is observed that with increasing the temperature, the formability also increases and specimens can be formed by lower loads. However, the trends of load–displacement curves become reversed when BHF is 14 kN and the effect of friction dominates the load curve trend, Fig. 17. Finally, the results showed that for the BHF of about 16 kN for Al 5052/SUS the effect of friction and formability can almost balance each other. The deformation mechanism for both cases of Al 1050/SUS and Al 5052/SUS are similar and the effects of various BHF on slide and plastic deformation for one sample of Al 5052/SUS are presented in Table 7. It can be concluded that increasing of BHF lead to reducing of sample slide and rising of plastic deformation.

### 3.5. Effect of grain size on load–displacement curve

Effect of grain size on load–displacement curves of Al 1050/SUS specimen is investigated here. The experiments are carried out for three different temperatures including 25 C, 100 C and 160 C. Fig. 18 represents the effect of different grain sizes of Al 1050 sheet on load–displacement curve for specimen of Al 1050/SUS with BHF of 15 kN. It is seen that the samples with higher grain size (14 μm) need more forming load when BHF is 15 kN. Formability, friction and BHF are

significant factors here which should be considered. When annealing temperature and grain size increase, some characteristics like strain hardening exponent, damage index and ductility also increase and accordingly the formability is enhanced. Hence, the improved ductility makes smaller the required forming load [2,29]. On the other hand, to determine the friction coefficient under various grain sizes for Al 1050 and Al 5052 sheets, the Coulomb friction test is performed in room temperature, Fig. 19. The results show that the grain size growth leads to increase of friction coefficient and in turn the forming load, Table 8. Similar to previous discussion, the BHF has a main role here to determine the dominating factor. Increasing or decreasing of forming load cannot be determined by the grain size solely, but the BHF has a significant role here and the trend of curves with different BHF is dissimilar. To clarify this, the experiments are re-carried out for BHF of 19, 17, and 15 kN, Fig. 20. As expected, trends of variations in load–displacement curves for tests with BHF of 15 and 19 kN are different which are reasonable. Furthermore, for the BHF of 17 kN, with larger grain size the forming load does not change and the effect of both factors can nearly balance each other. The details about sliding and plastic deformation are similar to pervious part and are presented in Table 6.

The effect of grain size on load–displacement curves for specimen of Al 5052/SUS also is investigated, Fig. 21. The trend of load–displacement curves for Al 5052/SUS are similar to Al 1050/SUS. The effect of BHF, which is again a crucial factor here, on Al 5052/SUS is presented in Fig. 22. In addition, the corresponding slide length and plastic deformation are also illustrated in Table 7.

## 4. Conclusion

To provide guidelines and to extend fundamental understanding of warm deep-drawing process on laminated sheets, some experimental tests were developed. The effects temperature, grain size, BHF, layer stacking sequence and friction as main factors influencing the load–displacement curves were investigated under various conditions of warm deep-drawing process and laminated sheets. In addition,

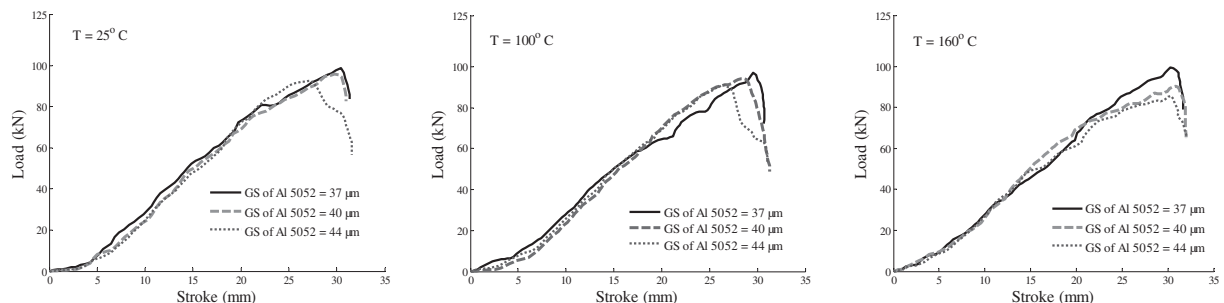


Fig. 21. Effect of various grain sizes of Al 5052 on load–displacement curve for specimen Al 5052/SUS when BHF = 18 kN.

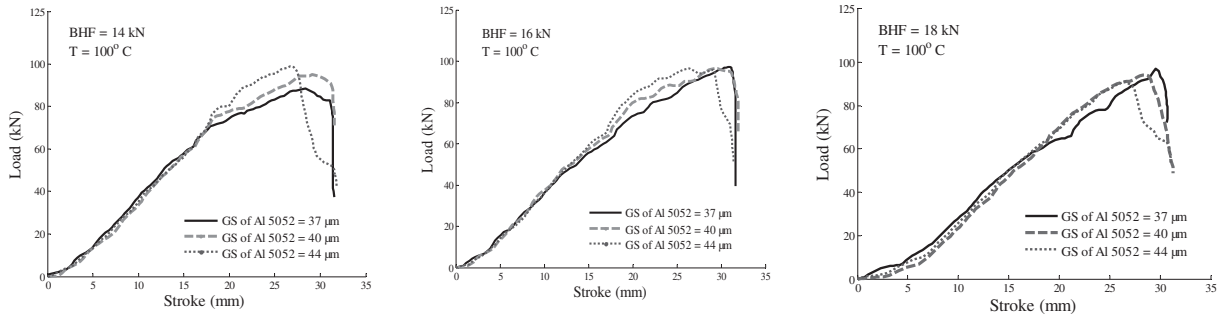


Fig. 22. Effect of various BHF on load–displacement curve for specimen Al 5052/SUS.

wrinkling and thinning for each layer were surveyed. The behaviors of Al 1050/SUS and Al 5052/SUS samples under various conditions were almost similar. In summary, the most important new results are as follows.

- (1) Re-crystallization takes place at the lowest investigated temperature of 350 C for aluminum sheets. Moreover, rising annealing temperature causes higher elongation, ultimate stress, yield stress, friction coefficient and grain size.
- (2) Distributions of thickness strain in the drawn cup indicates that the most susceptible regions to fracture in aluminum and stainless steel sheets are at the punch profile radius and central area of cup, respectively.
- (3) Compared to the aluminum sheets, number of wrinkles for stainless steel is more but with less amplitude. In addition, the average height of wrinkles for stainless steel sheets is more than that of aluminum sheets.
- (4) By changing the stacking sequence of layers, different forming loads are needed for forming, i.e. when stainless steel is placed as upper layer, less forming load is required rather than samples with aluminum as upper layer.
- (5) Two key factors with interaction effects are recognized, i.e. formability and friction coefficient. Both increase with rising temperature, however, the former decreases the required forming load and the latter increases it. Accordingly, the essential factor to analyze the forming load in various temperatures is the BHF. For instance, when decreasing the BHF the effect of friction became more significant. So that, with increasing blank temperature, the required load to form laminated sheet becomes higher. On the other hand, raising the BHF causes formability and plastic deformation and have dominant effects, which lead to warm deep-drawing process to be performed with less required load in higher temperatures.
- (6) Growth of grain size lead to increasing of formability and friction coefficient which have opposite effects on the process. Based on the aforementioned results, BHF plays a decisive role in this process, as well. When lower BHF is applied, the effect of friction becomes significant. Therefore, with larger grain size, the required load to form laminated sheet becomes higher. Nevertheless, higher BHF causes the effect of formability to become dominant. Hence, with larger grain size, the required load becomes less.

## References

- [1] F. Stachowicz, T. Trzepieciński, T. Pieja, Warm forming of stainless steel sheet, *Arch. Civ. Mech. Eng.* 10 (2010) 85–94.
- [2] K. Lange, K. Pöhlant, *Handbook of Metal Forming*, in: *Techniques Ingénieur* (Ed.), 1985.
- [3] H.-C. Tseng, C. Hung, C.-C. Huang, An analysis of the formability of aluminum/copper clad metals with different thicknesses by the finite element method and experiment, *Int. J. Adv. Manuf. Technol.* 49 (2010) 1029–1036.
- [4] S. Bagherzadeh, B. Mollaei-Darmani, K. Malekzadeh, Theoretical study on hydro-mechanical deep drawing process of bimetallic sheets and experimental observations, *J. Mater. Process. Technol.* 212 (2012) 1840–1849.
- [5] H. Takuda, K. Mori, H. Fujimoto, N. Hatta, Prediction of forming limit in deep drawing of Fe/Al laminated composite sheets using ductile fracture criterion, *J. Mater. Process. Technol.* 60 (1996) 291–296.
- [6] M.H. Parsa, K. Yamaguchi, N. Takakura, Redrawing analysis of aluminum–stainless-steel laminated sheet using FEM simulations and experiments, *Int. J. Mech. Sci.* 43 (2001) 2331–2347.
- [7] M.R. Morovvati, B. Mollaei-Darmani, M.H. Asadian-Ardakani, A theoretical, numerical, and experimental investigation of plastic wrinkling of circular two-layer sheet metal in the deep drawing, *J. Mater. Process. Technol.* 210 (2010) 1738–1747.
- [8] A. Atrian, F. Fereshteh-Saniee, Deep drawing process of steel/brass laminated sheets, *Compos. Part B* 47 (2013) 75–81.
- [9] A. Rajabi, M. Kadkhodayan, M. Manoochehri, R. Farjadfar, Deep-drawing of thermo-plastic metal-composite structures: experimental investigations, statistical analyses and finite element modeling, *J. Mater. Process. Technol.* 215 (2015) 159–170.
- [10] S. Toros, F. Ozturk, I. Kacar, Review of warm forming of aluminum–magnesium alloys, *J. Mater. Process. Technol.* 207 (2008) 1–12.
- [11] P. Bolt, N. Lambou, P. Rozier, Feasibility of warm drawing of aluminium products, *J. Mater. Process. Technol.* 115 (2001) 118–121.
- [12] H. Takuda, K. Mori, I. Masuda, Y. Abe, M. Matsuo, Finite element simulation of warm deep drawing of aluminium alloy sheet when accounting for heat conduction, *J. Mater. Process. Technol.* 120 (2002) 412–418.
- [13] Van den Boogaard AH, J. Hue 'tink, Simulation of aluminium sheet forming at elevated temperatures, *Comput. Methods Appl. Mech.* 195 (2006) 6691–6709.
- [14] G. Palumbo, L. Tricarico, Numerical and experimental investigations on the warm deep drawing process of circular aluminum alloy specimens, *J. Mater. Process. Technol.* 184 (2007) 115–123.
- [15] H.S. Kim, M. Koç, J. Ni, Development of an analytical model for warm deep drawing of aluminum alloys, *J. Mater. Process. Technol.* 197 (2008) 393–407.
- [16] H. Ibrahim Demirci, M. Yaşar, K. Demiray, M. Karalı, The theoretical and experimental investigation of blank holder forces plate effect in deep drawing process of AL 1050 material, *Mater. Des.* 29 (2008) 526–532.
- [17] M. El Sherbiny, H. Zein, M. Abd-Rabou, Thinning and residual stresses of sheet metal in the deep drawing process, *Mater. Des.* 55 (2014) 869–879.
- [18] H. Zein, M. El Sherbiny, M. Abd-Rabou, Thinning and spring back prediction of sheet metal in the deep drawing process, *Mater. Des.* 53 (2014) 797–808.
- [19] M. Ghosh, A. Miroux, R. Werkhoven, P. Bolt, L. Kestens, Warm deep-drawing and post drawing analysis of two Al–Mg–Si alloys, *J. Mater. Process. Technol.* 214 (2014) 756–766.
- [20] H. Takuda, K. Mori, T. Masachika, E. Yamazaki, Y. Watanabe, Finite element analysis of the formability of an austenitic stainless steel sheet in warm deep drawing, *J. Mater. Process. Technol.* 143–144 (2003) 242–248.
- [21] S.K. Singh, K. Mahesh, A. Kumar, M. Swathi, Understanding formability of extra-deep drawing steel at elevated temperature using finite element simulation, *Mater. Des.* 31 (2010) 4478–4484.
- [22] N. Ethiraj, V. Kumar, Finite element method based simulation on warm deep drawing of AISI 304 steel circular cups, *Procedia Eng.* 38 (2012) 1836–1851.
- [23] N. Ethiraj, V. Kumar, Experimental investigation on warm deep drawing of stainless steel AISI 304, *Appl. Mech. Mater.* 26 (2010) 436–442.
- [24] B. Bacroix, T. Chauveau, J. Ferreira Duarte, A. Barata da Rocha, J. Gracio, The respective influences of grain size and texture on the formability of a 1050 aluminium alloy, *Int. J. Eng. Sci.* 37 (1999) 509–526.
- [25] H. Rezaei Ashtiani, M. Parsa, H. Bisadi, Effects of initial grain size on hot deformation behavior of commercial pure aluminum, *Mater. Des.* 42 (2012) 478–485.
- [26] T. Lyman, *Metals Handbook: American Society for Metals*, 1967.
- [27] R.A. Morales, M.V. Candal, O.O. Santana, A. Gordillo, R. Salazar, Effect of the thermoforming process variables on the sheet friction coefficient, *Mater. Des.* 53 (2014) 1097–1103.
- [28] J. Coër, Mise en forme par emboutissage en température d'un alliage d'aluminium AA5754-O: Université de Bretagne Sud, 2013.
- [29] S.-H. Kang, Y.-S. Lee, H.W. Lee, Evaluation of flow stress and damage index at large plastic strain by simulating tensile test of Al6061 plates with various grain sizes, *Int. J. Mech. Sci.* 80 (2014) 54–61.